Supplementary Materials
Spinal Helical Actuation Patterns for Locomotion in Soft Robots

Jennifer C. Case, James Gibert, Joran Booth, Vytas SunSpiral, and Rebecca Kramer-Bottiglio

The Supplementary Materials contain the following sections:

S1. Component Fabrication

A. Spine

The spine consisted of two cylindrical structures that were fabricated from elastomer to incorporate flexibility into the structure of the robot. These elastomer sections of the cylindrical structures were designed to be 30 mm in diameter and 100 mm in length. The elastomer was molded with end caps (3D printed on a FormLabs stereolithography (SLA) printer) on either end that allowed the cylindrical structures to be connected together to form longer continuum structures or, in this case, the spine of the robot. Additionally, each end cap had dovetail insets that were used to attach and detach the robotic skins. These dovetail connections assist in transferring the forces between the skins and the underlying structure (i.e., the cylindrical structures). In the case of this legged robot, an additional leg connector was designed to fit between cylindrical structures and to hold the legs of the robot so that the legs did not need to be directly applied to the end caps. Two elastomers were used to create these cylindrical structures: Ecoflex 00-50 and Dragon Skin 10 Slow. Two cylindrical structures of each type of elastomer were fabricated for use as the spine of the robot.

B. Robotic Skins

The robotic skins were designed to fit around the previously described cylindrical structures of the spine. Robotic skins are fabricated from three components: a substrate, sensors, and actuators. The newly designed twisting skin used a $\approx$125 mm x 180 mm spandex fabric for the substrate. The basic layout of the skin is shown in Fig. 2. Iron-on reinforcements were cut out with a laser cutter (Universal Laser Systems) and applied where sensors, actuator attachments, and dovetail attachments were sewn onto the substrate. The sensors and actuator attachments were sewn on one side of the substrate while the dovetail attachments that fit into the dovetail insets of the cylindrical structures, were sewn on the opposite side. Both the actuator attachments and the dovetail attachments were 3D printed (FormLabs SLA printer). The sensors were made from an exfoliated graphite composite [1] and their manufacturing and construction have been explained previously [2], [3]. McKibben actuators with a braid diameter of 6.35 mm and a length of 140 mm were used in this work and their general construction has been explained previously [2]. These actuators were ziptied onto the actuator attachments to complete the skins. Similar to the skin presented by Case *et al.* [3], this skin has two horizontal sensors that could be used to measure the radius of the cylindrical structure that it is wrapped around as well as four sensors and actuators that run the length of structure. However, in this work, the sensors and actuators spiralled around the cylindrical structure rather than running parallel to the neutral axis. In the previous skins, button snaps have been used to close the skins around structures. With this skin design, the sensors and actuators formed a closed network since they encircle the entire skin (note that the blue and green dots map to each other in Fig. 2). Thus, the skin must be stretched over the cylindrical structure rather than wrapped around. Button snaps were still used in line with the horizontal sensors to ensure that they were in place properly.

C. Legs

The legs of this robot were designed to be unactuated and modular. Two leg designs were used: (1) rigid legs fabricated from 2.38 mm diameter brass tubing and (2) compliant legs fabricated from 1 mm diameter copper wire. The brass tubing legs were carefully manufactured to create three identical sets of legs to attach to the leg connectors, while the copper wire legs were wrapped directly onto the cylindrical structure's end caps and shaped by hand to approximately the same shape to simply highlight the difference between rigid and compliant legs with respect to torsional spinal-driven locomotion. The dimensions for the brass tubing legs are given in Fig. S1a and the average dimensions for the copper tubing legs are given in Fig. S1b. The legs were attached to the robot structure using hot glue because it held it in place, but was also meltable to rearrange if needed. Both legs were used on the robot, but most of the work studies the behavior with the rigid brass tubing legs due to their careful manufacturing.

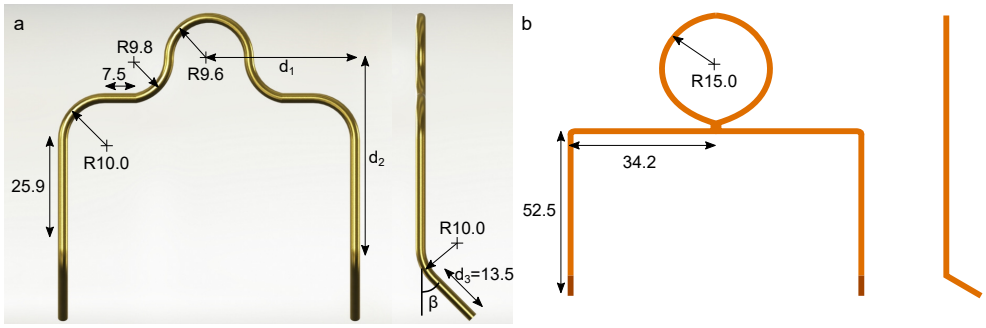

Fig. S1. (a) Dimensions of the brass tubing legs. (b) Average dimensions of the copper wire legs. Dimensions are given in mm.

S2. Spinal Gaits

The inflation patterns for each robotic skin are shown in Fig. S2 for the counter-twist gait and Fig. S3 for the bend-and-twist gait.

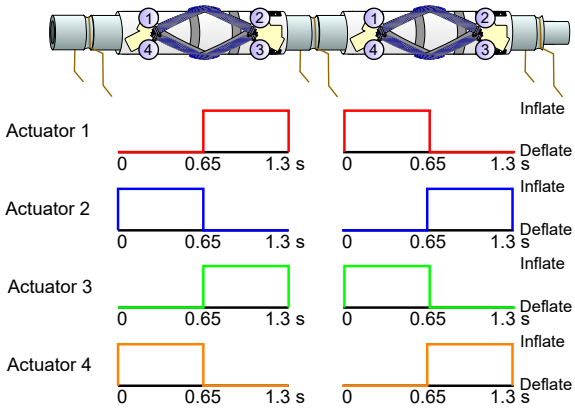

Fig. S2. Inflation and deflation patterns for the counter-twist spinal gait.

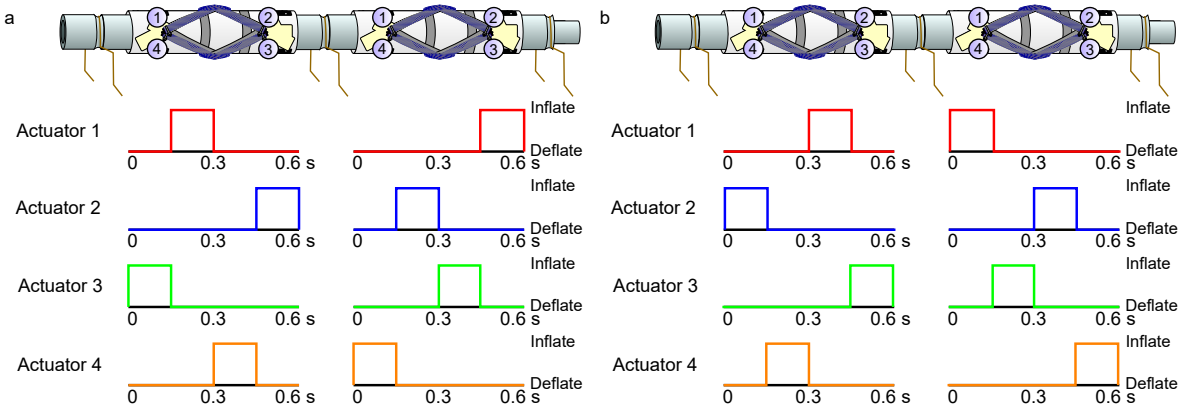

Fig. S3. Inflation and deflation patterns for the bend-and-twist spinal gait moving (a) forwards and (b) backwards.

S3. MODEL DERIVATION

In this section, we will walk through the entire derivation of the walking model of the robot that was used in the simulation. To start, we have approximated the forces from the actuators using,

$$F_1(t) = F_3(t) = \begin{cases} \frac{F_{max}}{t_1}(t - t_0) & 0 \leq t - t_0 < t_1 \\ -\frac{F_{max}}{t_2 - t_1}(t - t_0) + \frac{F_{max}}{t_2 - t_1}t_2 & t_1 \leq t - t_0 < t_2 \\ 0 & \text{otherwise} \end{cases}, \tag{S1a}$$

$$F_2(t) = F_4(t) = \begin{cases} \frac{F_{max}}{t_3 - t_2}(t - t_0) - \frac{F_{max}}{t_3 - t_2}t_2 & t_2 \leq t - t_0 < t_3 \\ -\frac{F_{max}}{t_4 - t_3}(t - t_0) + \frac{F_{max}}{t_4 - t_3}t_4 & t_3 \leq t - t_0 < t_4 \\ 0 & \text{otherwise} \end{cases}, \tag{S1b}$$

where F_{max} is the maximum force exerted by the actuators, t_i for $i = 1, 2, 3, 4$ are the time steps indicating inflation and deflation changes in the actuator, and t_0 is defined with Algorithm 1.

Algorithm 1: How to define t_0

```
t_0 = 0;
if (t - t_0) > t_4 then
    t_0 += t_4;
end
```

With the force fully defined, the axial compression force and moment that causes the cylindrical structure to twist can be found via Eqn. 1. With these equations known, the spinal stretch and maximum angle of twist can be found via Eqn. 5. Thus, we now have half of our state ($\mathbf{q}(t) = \{\lambda(t), \alpha(X_2, t), \mathbf{r}^{(1)}(t), \mathbf{r}^{(2)}(t)\}^T$) defined. The axes of rotations ($\mathbf{r}^{(i)}(t)$) change with respect to time as the robot deforms in order to keep the appropriate foot on the ground. To keep the foot on the ground, we assume $x_{planted,1} = P_{planted,1}$ and $x_{planted,3} = P_{planted,3}$ while letting $x_{planted,2}$ slide on the $\mathbf{e}_1$-$\mathbf{e}_3$ plane since the movement of $x_{planted,2}$ is what enables the forward locomotion of the robot. These boundary conditions combined with the knowledge that our axis is a unit vector gives us the following set of equations,

$$f_1 = P_{planted,1} - x_{planted,1} = (r_1^2 v_\alpha + c_\alpha - 1)P_1 + (r_1 r_2 v_\alpha - r_3 s_\alpha)(P_2 + \lambda X_2) + (r_1 r_3 v_\alpha + r_2 s_\alpha)P_3 = 0 \tag{S2a}$$

$$f_2 = P_{planted,3} - x_{planted,3} = (r_1 r_3 v_\alpha - r_2 s_\alpha)P_1 + (r_2 r_3 v_\alpha + r_1 s_\alpha)(P_2 + \lambda X_2) + (r_3^2 v_\alpha + c_\alpha - 1)P_3 = 0 \tag{S2b}$$

$$f_3 = \|\mathbf{r}^{(i)}\| - 1 = r_1^2 + r_2^2 + r_3^3 - 1 = 0 \tag{S2c}$$

where the planted foot and value of X_2 are defined by Eqn. 4. To figure out which foot is planted, the total gait is broken into four gait steps. The gait steps are defined with respect to time via Algorithm 2.

Algorithm 2: How to define the gait step

```
if (t - t_0) <= t_1 then
    Gait Step = 1;
    x_planted = P_{front,right};
else if t - t_0 <= t_2 then
    Gait Step = 2;
    x_planted = P_{rear,left};
else if t - t_0 <= t_3 then
    Gait Step = 3;
    x_planted = P_{front,left};
else
    Gait Step = 4;
    x_planted = P_{rear,right};
end
```

Due to the nonlinearity of Eqn. S2, finding a solution for $\mathbf{r}^{(i)}$ was found numerically using Newton's method,

$$\mathbf{r}_{n+1} = \mathbf{r}_n - \mathbf{J_F}(\mathbf{r}_n)^{-1}\mathbf{F}(\mathbf{r}_n), \tag{S3}$$

where $\mathbf{F} = \{f_1, f_2, f_3\}^T$ and $\mathbf{J_F}$ is the Jacobian of $\mathbf{F}$ and can be written as,

$$\mathbf{J_F}(\mathbf{r}) = \begin{bmatrix} 2r_1 v_\alpha P_1 + r_2 v_\alpha (P_2 + \lambda X_2) + r_1 v_\alpha P_3 & r_1 v_\alpha (P_2 + \lambda X_2) + s_\alpha P_3 & -s_\alpha (P_2 + \lambda X_2) + r_1 v_\alpha P_3 \\ r_3 v_\alpha P_1 + s_\alpha (P_2 + \lambda X_2) & -s_\alpha P_1 + r_3 v_\alpha (P_2 + \lambda X_2) & r_1 v_\alpha P_1 + r_2 v_\alpha (P_2 + \lambda X_2) + 2 r_3 v_\alpha P_3 \\ 2r_1 & 2r_2 & 2r_3 \end{bmatrix}. \tag{S4}$$

This Jacobian is invertible as long as $\alpha \neq 0$. If $\alpha = 0$, we can define $\mathbf{r}^{(1)} = \{0, -1, 0\}$ and $\mathbf{r}^{(2)} = \{0, 1, 0\}$, which also serve as the initial guesses in our Newton's method. The Newton's method is run until $\sum f_i < \delta$, where δ is a user-defined tolerance, or until the number of iterations exceeds a maximum user-defined iteration value.

The step size between time steps is found through Eqn. 6 and is used to translate the robot's position from the local coordinate frame to the global coordinate frame via,

$$\mathbf{T}_{global}(t) = \mathbf{T}_{global}(t-1) + \mathbf{u}(t), \tag{S5}$$

where T_{global} is the translation from the local coordinate frame to the global coordinate frame. The global position is found via,

$$\mathbf{x}_{global}(t) = \mathbf{x}(t) + \mathbf{T}_{global}(t), \tag{S6}$$

where $\mathbf{x}_{global}$ is the position in the global coordinate frame.

S4. Simulation Example: Matching Simulation to EcoFlex 00-50 Robot

The goal of this example is to demonstrate how the simulation works. For this example, we have chosen to approximate the performance of the EcoFlex 00-50 physical robot with an EcoFlex 00-50 simulated robot. The parameter values for the elastomer sections and the legs are given in Tables S1 and S2, respectively.

TABLE S1
Parameters for the Elastomer Sections of the Simulated Robot

Parameter	Value
Length	100 mm
Radius	15 mm
Elastic Modulus	122 kPa
Poisson Ratio	0.5
Actuator Angle	26.5°

TABLE S2
Parameters for the Legs of the Simulated Robot

Parameter	Value
d_1	73.8 mm
d_2	25.9 mm
d_3	13.5 mm
β	45°

The forces of the actuators are defined with Eqn. S1 and the parameters given in Table S3. The times for the simulated robot are chosen such that we approximate the times where one set of actuators is inflating while the others are deflating on the physical robot. The force is additionally defined by a maximum time of 10 s with a step size of 0.01 s. It is important that the step size is able to capture the values of t_i for $i = 1, 2, 3, 4$ or there can be jumps in the calculation of the force. The actuator forces for this robot are shown in Fig. S4.

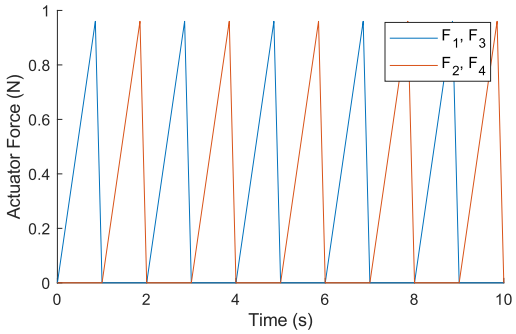

Fig. S4. Force response from each actuator given Eqn. S1 and the parameters in Table S3.

With the actuator forces known, the compression force, moment that causes the cylindrical structure to twist, stretch, and maximum angle of twist can be calculated. The values of these variables are shown in Fig. S5.

When calculating the deformation of the robot, the stretch, maximum angle of twist, and gait step are calculated. Next, we start tracking the translation between the global and local coordinate frames. To do this, start by defining where we want the

TABLE S3
PARAMETERS FOR THE ACTUATOR FORCES OF THE SIMULATED ROBOT

Parameter	Value
F_{max}	0.96 N
t_1	0.85 s
t_2	1 s
t_3	1.85 s
t_4	2 s

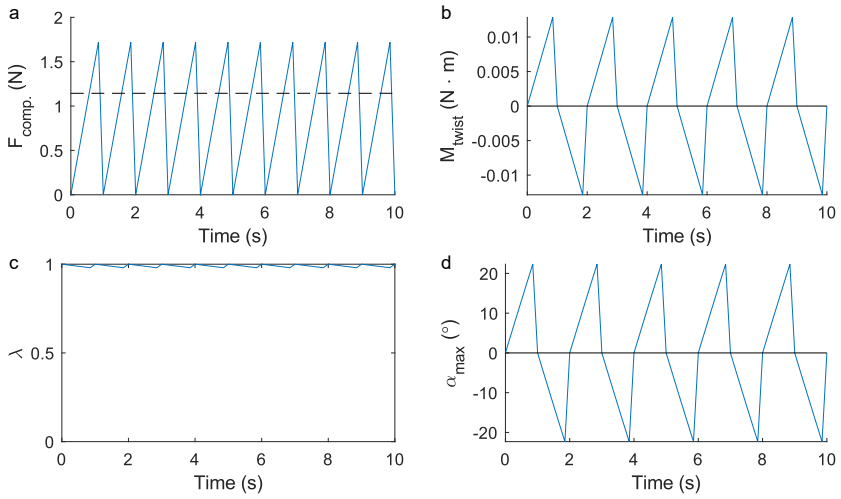

Fig. S5. (a) The compression force experienced by each elastomer section is shown in blue. The buckling force of the elastomer section is shown as a black dashed line. (b) The moment response on the elastomer section caused by the actuator forces. (c) The stretch response due to the compression force. (d) The maximum angle of twist on the elastomer sections as a function of the stretch and moment response.

feet to start in the global frame. For this system, I selected to have the robot walk on the $\mathbf{e}_1$-$\mathbf{e}_2$ plane, which means that the translation is given by,

$$\mathbf{T}_{global}(t=0) = \{0, 0, d_2 + d_3 \cos\beta, 0\}^T. \tag{S7}$$

Since $F_i = 0$ for $i = 1, 2, 3, 4$ initially, we know that $\alpha_{max} = 0$. Thus, we set,

$$\mathbf{r}^{(1)}(t=0) = \{0, -1, 0\}, \tag{S8a}$$

$$\mathbf{r}^{(2)}(t=0) = \{0, 1, 0\}. \tag{S8b}$$

Since the Newton's method requires an initial guess, we use the result from the previous time step ($\mathbf{r}^{(i)}(t-1)$) as the initial guess for the current time step. A tolerance of $\delta = 10^{-6}$ and a maximum iteration of 1000 was used for the Newton's method.

Finally, we use Eqn. 6 to calculate the step size to update the translation between the local and global coordinate frames. Fig. S6 shows a comparison between the simulation and physical robot at various time steps.

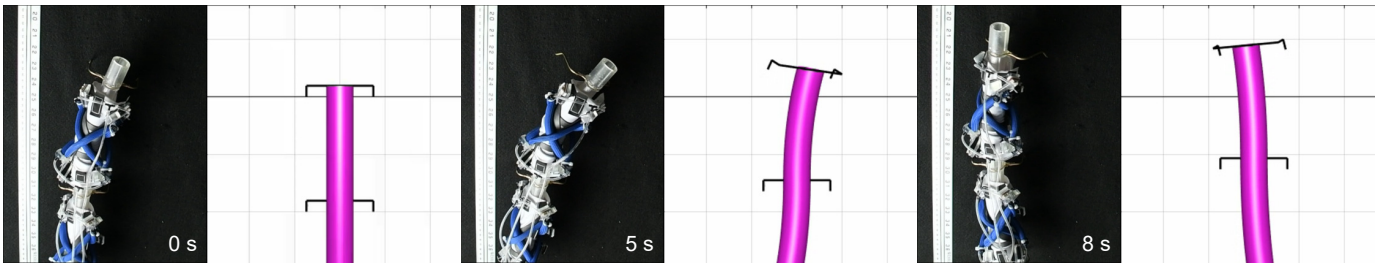

Fig. S6. Side-by-side comparison of the physical robot and the simulated robot.

REFERENCES

[1] E. L. White, M. C. Yuen, J. C. Case, and R. K. Kramer, "Low-Cost, Facile, and Scalable Manufacturing of Capacitive Sensors for Soft Systems," *Advanced Materials Technologies*, vol. 2, no. 9, p. 1700072, 2017.

[2] J. C. Case, J. Booth, D. S. Shah, M. C. Yuen, and R. Kramer-Bottiglio, "State and stiffness estimation using robotic fabrics," in *2018 IEEE International Conference on Soft Robotics (RoboSoft)*, pp. 522–527, Apr. 2018.

[3] J. C. Case, M. C. Yuen, J. Jacobs, and R. Kramer-Bottiglio, "Robotic Skins That Learn to Control Passive Structures," *IEEE Robotics and Automation Letters*, vol. 4, pp. 2485–2492, July 2019.